Multiporosity Flow of Gases in Fractured Shale Formations

Kristopher L. Kuhlman[1], Jason E. Heath, W. Payton Gardner, and David G. Robinson

[1]klkuhlm@sandia.gov AGU Fall Meeting 2014 H51B-0610 Sandia National Laboratories†, Albuquerque, New Mexico

Hydrocarbon wells in low-permeability shales are complex. We are using naturally occurring noble gas tracers in hydraulically fractured shale wells to increase the total information available for parameter estimation and uncertainty analysis.

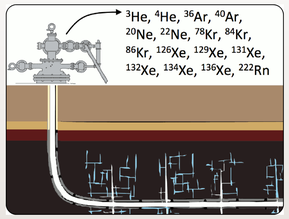

Helium and other noble gases may exist in high concentrations in hydrocarbon reservoirs as by-products of radioactive decay of natural uranium and thorium. Helium is a small inert molecule, and the noble gases (He, Ne, Ar, Kr, Xe & Rn) have a wide range of molecular sizes, diffusion coefficients, and propensities to sorb onto organic matter.

Naturally occurring tracers are brought to the borehole through advection (due to a uniform initial concentration), driven by pressure gradients. Different species may have their own effective permeabilities, porosities, and compressibilities – helium being the most favorable, because it is a small inert molecule.

Multiporosity Flow Model

We extend the classical *double porosity* flow model [8] to a single fracture continuum and N matrix continua using the multirate transport approach [5].

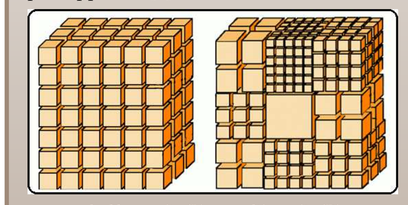

double porosity (L) vs. multiporosity (R)

The fracture flow equation ($_f$ denotes fracture continuum) is

$$\omega_f \frac{\partial \psi_f}{\partial t_D} + \sum_{j=1}^{N} \omega_j \chi_j \frac{\psi_j}{\partial t_D} = \nabla^2 \psi_f, \qquad (1)$$

where ψ_f is the dimensionless pressure head change [L], $\omega_\ell = \frac{c_\ell \phi_\ell}{c_f \phi_f + \sum c_j \phi_j}$, $\ell = \{f, 1, \ldots, N\}$ is a storage capacity ratio (c is formation compressibility [L^{-1}] and ϕ is porosity), $t_D = t/(r_w^2 \mu \phi c_f / k_f)$ is dimensionless time, μ is fluid viscosity [LT], r_w is wellbore radius [L], and χ is a dimensionless probability mass function (a discrete probability distribution).

The matrix flow equation (j denotes matrix continua) is

$$\omega_j \frac{\partial \psi_j}{\partial t_D} = \kappa_j \nabla^2 \psi_j \qquad j = 1, \ldots, N, \qquad (2)$$

where $\kappa_j = k_j/k_f$ is the matrix/fracture permeability ratio.

Integrating (2) across an assumed one-dimensional matrix perpendicular to the fracture (see coordinate convention in diagram at top of center column) produces

$$\frac{\partial \langle \psi_j \rangle}{\partial t_D} = \frac{\kappa_j}{y_{eD} \omega_j} \left[\left. \frac{\partial \psi_j}{\partial y_D} \right|_{y_D = y_{eD}} - \left. \frac{\partial \psi_j}{\partial y_D} \right|_{y_D = 0} \right],$$

where $\langle \psi_j \rangle(t) = \frac{1}{y_{eD}} \int_0^{y_{eD}} \psi_j(y, t)\, \mathrm{d}y$ is the spatially averaged change in matrix pressure.

The pseudo steady-state interporosity flow approximation (used by [3] & [8]) assumes flow to or from the matrix is proportional to their difference in fracture and matrix pressures

$$\frac{\partial \langle \psi_j \rangle}{\partial t_D} = \frac{\alpha_j \kappa_j r_w^2}{\omega_j} [\psi_f - \psi_j] \qquad j = 1, \ldots, N, \qquad (3)$$

where α_j is the Warren & Root "shape parameter" [L^{-2}].

We use the Laplace transform to solve the matrix (3) and fracture (1) governing equations simultaneously, leading to:

$$\left[1 + \sum_{j=1}^{N} \frac{\omega_j}{\omega_f} \frac{u_j \chi_j}{s + u_j} \right] s \bar{\psi}_f = \nabla^2 \bar{\psi}_f, \qquad (4)$$

where $u_j = \alpha_j \kappa_j r_w^2 / \omega_j$ is the summation parameter characterizing the matrix (also the abscissa for the probability mass function χ_j), s is the dimensionless Laplace parameter and an overbar indicates a Laplace-transformed variable. The time-domain results are computed using a numerical inverse Laplace transform [4]. The bracketed quantity (η^2) in (4) is the modified Helmholtz wave number [1].

The multiporosity model can generalize the dual porosity Warren & Root [8] pseudo-steady-state interporosity flow model ($N = 1$), triple-porosity pseudo-steady state interporosity flow models [3] ($N = 2$), and can approximate the transient interporosity flow model of Kazemi [6] ($N \to \infty$). Adapting results from [5], the series

$$u_j = (2j-1)^2 \pi^2 y_{eD}^2 \alpha_j \kappa_j / (4\omega_j)$$
$$\chi_j = 8\omega_j / \left[(2j-1)^2 \omega \pi_j \right]$$

with $j = 1, \ldots, \infty$ can be used to approximate transient diffusion into the matrix with an infinite series of pseudo steady-state porosities.

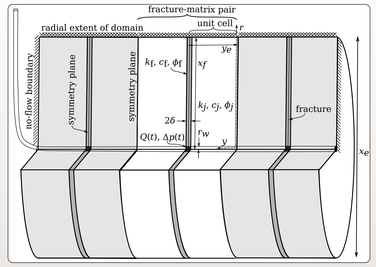

Radially symmetric well test solution geometry showing fracture, matrix, and "unit cell"

Radial Well Test Solutions

We solve the governing equation (4) in radial coordinates for two wellbore boundary conditions, for both infinite and finite domains with a general Type-III boundary condition at the radial extent of the domain.

The Laplace-domain specified flowrate solution in an infinite domains is

$$\bar{\psi}_f^{(q,\infty)} = \frac{\mathrm{K}_0(\eta)}{s\mathrm{K}_1(\eta)}$$

where K is a modified Bessel function. The specified downhole pressure solution for an infinite domain is

$$\bar{q}_f^{(P,\infty)} = \pi \delta_D \eta \frac{\mathrm{K}_1(\eta)}{s\mathrm{K}_0(\eta)}$$

where δ_D is the dimensionless fracture aperture.

For a finite domain the specified flowrate solution is

$$\bar{\psi}_f^{(q,x_f)} = \frac{1}{s\eta} \frac{\mathrm{I}_0(\eta)\xi + \mathrm{K}_0(\eta)\zeta}{\mathrm{I}_1(\eta)\xi - \mathrm{K}_1(\eta)\zeta}$$

and the finite domain solution for specified bottomhole pressure is

$$\bar{q}_f^{(P,x_f)} = \frac{\pi \delta_D \eta}{s} \frac{\mathrm{I}_1(\eta)\xi - \mathrm{K}_1(\eta)\zeta}{\mathrm{I}_0(\eta)\xi + \mathrm{K}_0(\eta)\zeta}$$

where

$$\xi = \eta \mathrm{K}_1(\eta x_{fD}) - H_D \mathrm{K}_0(\eta x_{fD}),$$
$$\zeta = \eta \mathrm{I}_1(\eta x_{fD}) + H_D \mathrm{I}_0(\eta x_{fD}),$$

I is a modified Bessel function, and H_D is a dimensionless boundary conductance. The limiting value of $H_D = 0$ makes the Type-III boundary no-flow (Type II), $H_D \to \infty$ makes the boundary constant head (Type I).

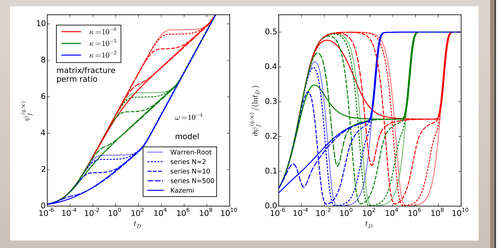

Predicted pressure (L) and derivative (R) for specified flowrate multiporosity solution

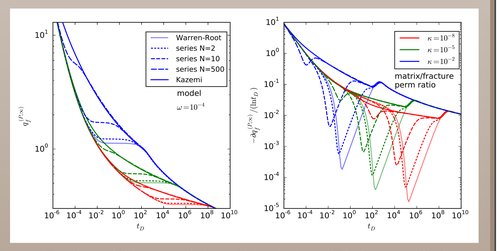

Predicted flowrate (L) and derivative (R) for specified bottomhole pressure multiporosity solution

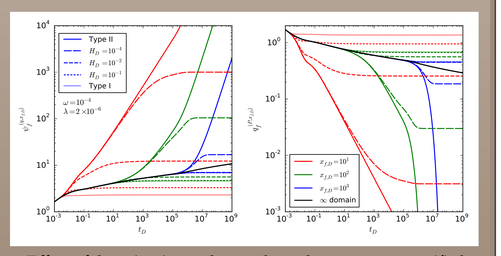

Effect of domain size and outer boundary type on specified flowrate (L) and bottomhole pressure (R) response

Natural Gas Production Data

Transient pressure and gas, oil, and water production data collected from the wellhead at hydrofractured horizontally completed natural gas wells (upper left figure) are used to approximate down-hole pressure and flowrate using the ideal gas law and wellbore mass and energy balances [7] (upper right figure). Choke is plotted on the right axis in each figure, and represents the size of the opening on the surface through which the fluids are allowed to flow. Because gas is highly compressible, a pseudo-potential must be computed (lower right figure),

$$\Delta m = \int_{p_0}^{p_1} \frac{p}{\mu_g Z} \mathrm{d}p \qquad t_a = \mu_g c \int_0^t \frac{\mathrm{d}t}{\mu_g c}$$

where $\mu_g(p, T)$ is the pressure- and temperature-dependent gas viscosity, $Z(p, T)$ is the ideal gas deviation factor, m is a pseudo-pressure, and t_a is a pseudo-time [2].

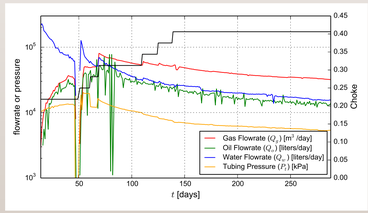

Gas well production data

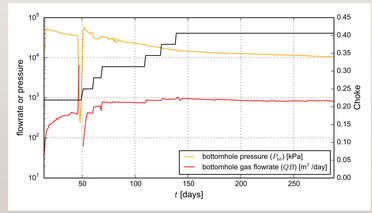

Computed bottom-hole pressure and production

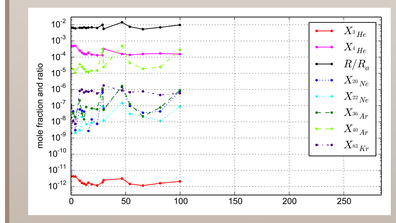

Noble gas isotope mole fraction data

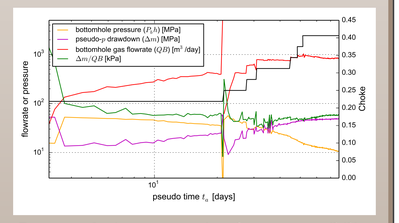

Pressure & time accounting for compressibility

Gases from hydrocarbon wells have recently been sampled and analyzed for noble gas content (lower left figure), but definitive analysis is waiting on more noble gas data.

We are developing more realistic wellbore and production models to capture the early production data (taking the applied choke into account) as shown in upper left figure above. The early peak of water production (blue), followed by a delayed peak in gas (red) and oil (green) production are unique to hydrofractured shale wells. They are representative of the multi-phase interaction of fluids in both the fracture and matrix after high-pressure water injection.

We are combining development of physically realistic fractured rock models, realistic wellbore production models, and noble gas flow and transport data in a Bayesian framework, to improve understanding of gas flow in low-permeability formations.

[1] M. Bakker and K. L. Kuhlman. Computational issues and applications of line-elements to model subsurface flow governed by the modified Helmholtz equation. *Advances in Water Resources*, 34(9):1186–1194, 2011.

[2] C. R. Clarkson. Production data analysis of unconventional gas wells: Review of theory and best practices. *International Journal of Coal Geology*, 109–110:101–146, 2013.

[3] P. J. Clossman. An aquifer model for fissured reservoirs. *Soc. Pet. Eng. J. Trans. AIME*, 259:385–398, 1975.

[4] F. R. de Hoog, J. H. Knight, and A. N. Stokes. An improved method for numerical inversion of laplace transforms. *SIAM J. on Sci. and Stat. Comp.*, 3(3):357–366, 1982.

[5] R. Haggerty and S. M. Gorelick. Multiple-rate mass-transfer for modeling diffusion and surface-reactions in media with pore-scale heterogeneity. *Water Resources Research*, 31(10):2383–2400, 1995.

[6] H. Kazemi. Pressure transient analysis of naturally fractured reservoirs with uniform fracture distribution. *SPE Journal*, 9(4):451–462, 1969.

[7] R. D. Oden and J. W. Jennings. Modification of the Cullender and Smith equation for more accurate bottomhole pressure calculation in gas wells. In *Permian Basin Oil and Gas Recovery Conference, Midland TX*, 1988.

[8] J. E. Warren and P. J. Root. The behavior of naturally fractured reservoirs. *SPE Journal*, 3(3):245–255, 1963.

† Sandia National Laboratories is a multi-program laboratory managed and operated by Sandia Corporation, a wholly owned subsidiary of Lockheed Martin Corporation, for the U.S. Department of Energy's National Nuclear Security Administration under contract DE-AC04-94AL85000.

Exceptional service in the national interest